

# Scalable Synthesis of Switchable Assemblies of Gold Nanorod Lyotropic Liquid Crystal Nanocomposites

Xiao Liu, Genggeng Qi, Albert Min Gyu Park, Arnaldo Rodriguez-Gonzalez, Apostolos Enotiadis, Wenyang Pan, Vasiliki Kosma, Gregory D. Fuchs, Brian J. Kirby, and Emmanuel P. Giannelis\*

**A new class of solvent free, lyotropic liquid crystal nanocomposites based on gold nanorods (AuNRs) with high nanorod content is reported. Application of shear results in switchable, highly ordered alignment of the nanorods over several centimeters with excellent storage stability for months. For the synthesis, AuNRs are surface functionalized with a charged, covalently tethered corona, which induces fluid-like properties. This honey-like material can be deposited on a substrate and a high orientational order parameter of 0.72 is achieved using a simple shearing protocol. Switching shearing direction results in realignment of the AuNRs. For a film containing 75 wt% of AuNRs the alignment persists for several months. In addition to the lyotropic liquid crystal characteristics, the AuNRs films also exhibit anisotropic electrical conductivity with an order of magnitude difference between the conductivities in direction parallel and perpendicular to the alignment of the AuNRs.**

For more than a decade, gold nanoparticles have been used in a wide variety of high-tech fields, such as energy harvesting and storage, catalysis, optics, and biomedicine due to their exceptional optical, electronic, and biocompatible properties.<sup>[1–12]</sup> In particular, gold nanorods (AuNRs) have been receiving increasing attention from many fields of science and technology because of their distinct localized surface plasmonic characteristics, which are easily tuned by varying the aspect ratio of AuNRs.<sup>[13–16]</sup> It is noteworthy that the assembly of AuNRs into ordered superstructures results in significant enhancement of surface-enhanced Raman scattering and luminescence, and

thus, it has found numerous applications, such as nanoantennae, surface-enhanced Raman spectroscopy, and switchable optical metamaterials.<sup>[17–24]</sup>

Over the past few years several methods have been developed to prepare ordered AuNRs assemblies. One commonly used method is evaporation-induced self-assembly of AuNRs, which is known for its cost-effectiveness and versatility. Peng et al. fabricated patterned arrays of millimeter scale plasmonic superlattices composed of nearly vertically aligned AuNRs by evaporation of surface functionalized AuNRs.<sup>[18]</sup> In addition, Yin et al. prepared vertically aligned AuNRs monolayer supercrystals, which increased the upconversion luminescence intensity of NaYF<sub>4</sub>:Yb<sup>3+</sup>, Er<sup>3+</sup> nanocrystals more than


35 fold.<sup>[24]</sup> However, the complex drying mechanisms and interactions between particles, particle-solvent, and particle-substrate involved in the evaporation process pose a great challenge in precisely controlling the long-range structure of AuNRs, particularly over a large-scale area. Aiming to address this challenge, topographical substrates have been used to achieve a large-scale organization of AuNRs with controlled position, orientation, and interparticle distance. Such patterns are generated using block copolymers, lithography, or wrinkled polydimethylsiloxane as templates.<sup>[25–27]</sup>

A major limitation for methods above is that they lack the possibility for nanorod switching to make a switchable AuNR film. The tunability of an assembly of nanorods is crucial for optical and electric applications such as tunable linear-polarized light emitters and tunable polarizer filters, tunable diodes, shear sensors, and stretch detectors. In this respect, the use of directional molecular or polymeric templates, such as liquid crystals and surfactant micelles, has shown promising results so far. Feng et al.<sup>[28]</sup> and Rozic et al.<sup>[29]</sup> functionalized AuNRs with liquid crystal ligands and achieved macroscopic alignment after shearing. Liu et al. reported the self-alignment of dispersed gold nanorods guided by the micelles in nematic and hexagonal liquid crystalline phases.<sup>[30]</sup> Mirkin et al. used DNA as a programmable linker to assemble functionalized AuNRs into a hexagonal 2D layer.<sup>[31]</sup> However, systems with a low AuNR weight ratio are typically used, which may pose limitations to certain applications such as high-efficiency nanoantennas, conductive inks, printable electronics, and

X. Liu, Dr. G. Qi, Dr. A. Enotiadis, Dr. W. Y. Pan, Dr. V. Kosma, Prof. E. P. Giannelis  
Materials Science and Engineering  
Cornell University  
Ithaca, NY 14853, USA  
E-mail: epg2@cornell.edu

A. M. G. Park, Prof. G. D. Fuchs  
School of Applied and Engineering Physics  
Cornell University  
Ithaca, NY 14853, USA

A. Rodriguez-Gonzalez, Prof. B. J. Kirby  
Sibley School of Mechanical and Aerospace Engineering  
Cornell University  
Ithaca, NY 14853, USA

 The ORCID identification number(s) for the author(s) of this article can be found under <https://doi.org/10.1002/sml.201901666>.

DOI: 10.1002/sml.201901666

photovoltaics. In addition to these methods, some other methods have been developed to fabricate AuNR assemblies, which use external fields, such as grazing incidence spraying and flow assembly.<sup>[32,33]</sup> However, for practical applications of AuNRs, a simple process that yields a high degree of alignment is desirable. The scalable assembly of AuNRs with high nanorod content that can be realigned multiple times with long-term storage stability is still a challenge.

Recently, nanoscale ionic materials (NIMs) with tunable rheological behavior were developed in our group.<sup>[34–37]</sup> NIMs consist of nanoparticle cores functionalized with a charged corona, which is balanced by a counter-ion canopy. The ionic nature of NIMs endows them a fluid-like behavior under ambient conditions and in the absence of solvents.<sup>[38]</sup> By properly engineering the nanoparticle core, corona, and canopy, it is possible to fine-tune the rheological behavior of NIMs and in some cases to switch and retain any alignment under ambient conditions. Moreover, the strong ionic interaction between the core and the canopy prevents microphase separation.<sup>[36]</sup> Therefore, NIMs appear as a good candidate for scalable production of switchable assemblies. Our group has previously used poly(sodium 4-styrenesulfonate) (PSS) to synthesize AuNR NIMs and achieved alignment by shearing; nevertheless, the weight ratio of AuNRs and the degree of alignment remained a challenge.<sup>[39]</sup> Thus, we sought to develop a better way to synthesize AuNR NIMs to improve those properties.

In this paper, we describe a facile and versatile approach to prepare AuNR assemblies over centimeter-scale areas based on NIMs. Even with a high AuNR weight ratio of 75%, an order of magnitude larger than that of switchable assemblies previously reported,<sup>[28,30]</sup> alignment of AuNRs over centimeters can be accomplished simply by shearing.

The AuNRs were synthesized by the seed-mediated method,<sup>[40]</sup> using hexadecyltrimethylammonium bromide (CTAB) and sodium oleate (NaOL) as the capping ligands (Figure 1a). The as-synthesized AuNRs have an average diameter of 10 nm and average length of 80 nm (Figure 1b). The bilayer of partially interdigitated CTAB molecules produces a positively charged shield around the AuNRs preventing them from aggregation. Sodium 3-mercapto-1-propanesulfonate (MPS) was used to replace the surface adsorbed CTAB/NaOL molecules in order to develop ionic functionality composed of sulfonic groups and facilitate the formation of the AuNR NIMs (Figure 1a). Since direct ligand exchange of CTAB with MPS causes irreversible aggregation of AuNRs due to surface charge neutralization of AuNRs and the destruction of the CTAB bilayer, a new method was developed. To that end, PSS was used as an intermediate ligand to stabilize the AuNRs via steric stabilization mechanism.<sup>[41,42]</sup> Then, the protonated MPS ligands neutralized by the amine terminated PEG oligomer (Jeffamine) was used to replace PSS and hexadecyltrimethylammonium bromide (CTBA) molecules. The obtained MPS-Jeffamine functionalized AuNRs were freeze dried to give the AuNR NIMs with fluid-like property.

The successful synthesis of ionic AuNR NIMs was confirmed by surface characterization using zeta potential measurements and X-ray photoelectron spectroscopy (XPS). After the ligand exchange with PSS, positively charged CTBA-AuNRs ( $\zeta = +44 \pm 2$  mV) became strongly negative ( $\zeta = -31 \pm 2$  mV).

As shown in Figure 1c, after the ligand exchange with MPS-Jeffamine, an Au-S 2p peak was observed in the high resolution XPS spectrum indicating the presence of a bond between MPS-Jeffamine and AuNRs surface.<sup>[43]</sup>

Figure 1d shows the thermogravimetric analysis (TGA) profile of AuNR NIMs with  $\approx 75$  wt% of AuNR content. The AuNR NIMs exhibit good thermal stability up to 200 °C. The sharp weight loss between 300 and 400 °C results from the decomposition of Jeffamine. Figure 1e shows the transmission electron microscope (TEM) images of AuNR NIMs, which demonstrates the random alignment of AuNRs before shearing. The NIMs containing 75% AuNRs appear as a thick, honey-like viscous liquid, and its viscosity decreases sharply under shearing (Figure S1, Supporting Information). After deposition on a substrate, a uniform thin film is formed. The film can be aligned by shearing the AuNR NIMs using a glass coverslip at a shear rate  $\approx 200$  s<sup>-1</sup> (Figure S2, Supporting Information).

The alignment of AuNR NIMs was studied via polarized optical microscopy (POM) and linearly polarized UV spectrometry. The AuNR NIMs were placed between two glass slides and aligned by simply shearing the upper slide in one direction. The alignment of AuNR NIMs is switchable by shearing in the orthogonal direction (Figure 2a). We note that alignment was achieved for systems containing 75% AuNRs by weight, which is ten times higher than that of the AuNRs assemblies with switchable alignment previously reported.<sup>[28,30]</sup> Figure 2b,c shows the POM images of the aligned AuNR NIMs film before and after altering the direction of shearing. The aligned film exhibited the strongest birefringence (Figure 2b,c), when the shearing direction was at  $\approx 45^\circ$  with respect to the polarizer. When the polarizer was parallel to the shearing direction, the film showed the weakest birefringence (Figure S3a, Supporting Information). The strong birefringence over centimeters seen in Figure 2b,c indicates long-range alignment of AuNRs along the shearing direction. A nonionic, control sample prepared by dispersing unprotonated (e.g., the sodium form of) MPS functionalized AuNRs with Jeffamine was used for comparison. The lack of acid-base interactions between the MPS and Jeffamine prevents the formation of an ionic NIMs-like system. The film generated using the control sample showed much weaker birefringence at  $45^\circ$  (Figure 2d,e) and noticeable birefringence when the polarizer was parallel to the shearing direction (Figure S3b, Supporting Information). These results indicate that the ionic interaction plays an essential role for efficient nanorod alignment.

Polarized UV spectrometry was used to further investigate the alignment of AuNRs in the NIMs film. In the optical spectroscopy measurement, the sample was fixed on the stage and the polarizer was rotated so that the probing light always passed through the same area of the film. The absorption spectrum of an aqueous dispersion of AuNRs (without any directional alignment due to Brownian motion) exhibits polarization-independent transverse and longitudinal surface plasmon resonance (SPR) peaks (Figure S4a, Supporting Information). In contrast, the absorption spectrum of aligned AuNR NIMs film changed upon varying the angle between the polarizer and the shearing direction. The SPR peak of the AuNR NIMs film is broader compared to that of the pristine AuNRs in water (Figure S4, Supporting Information). We attribute this

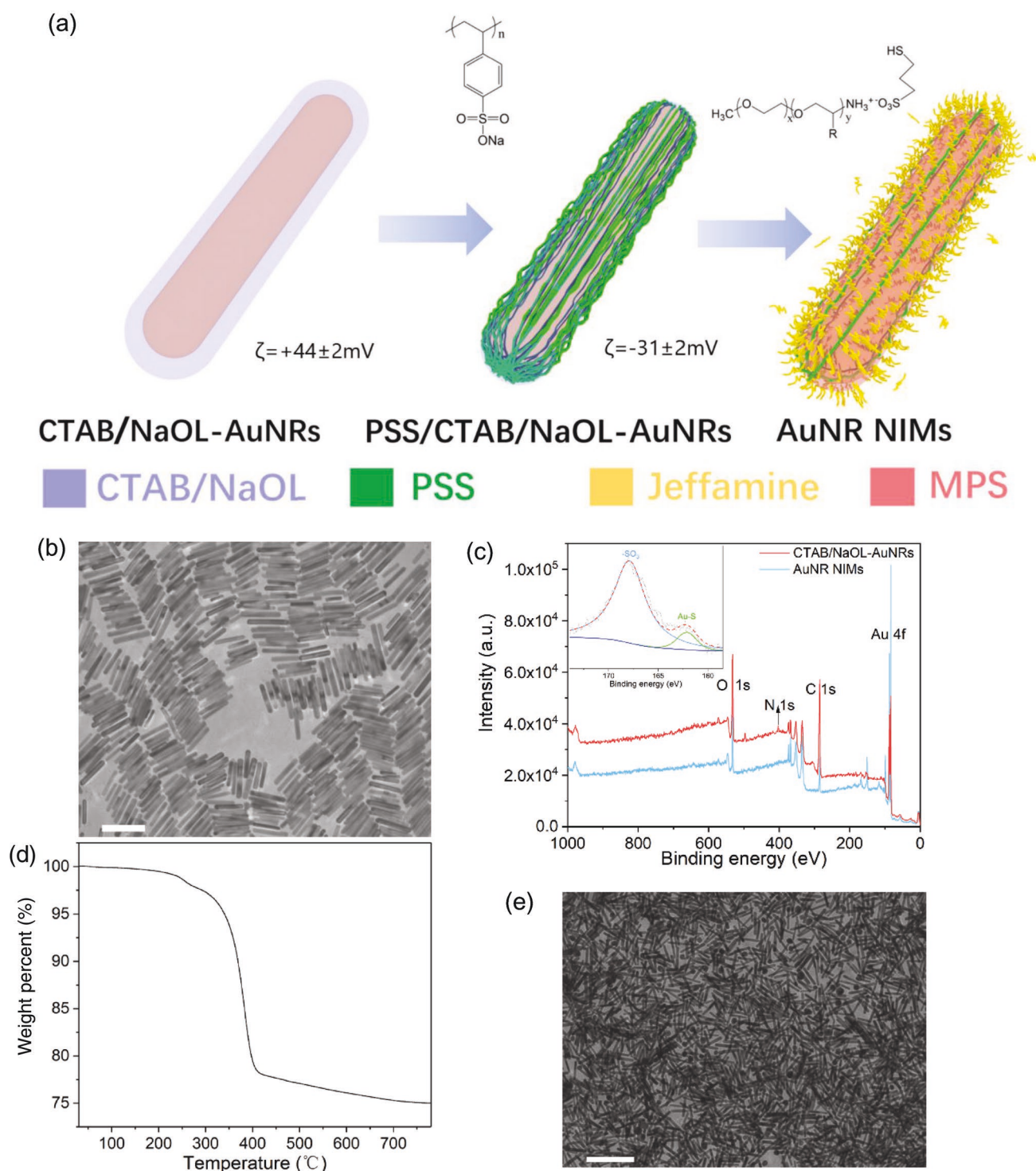


**Figure 1.** a) Schematic diagram of synthesis of the AuNR NIMs with Jeffamine as the canopy. b) TEM microscopic images of CTAB/NaOL-AuNRs (scale bar = 100 nm). c) XPS spectra of the CTAB/NaOL-AuNRs and AuNR NIMs. Inset: high-resolution XPS of the S region. d) Thermogravimetric analysis profile of AuNR NIMs containing 75 wt% of AuNRs. e) TEM micrograph of AuNR NIMs (scale bar = 200 nm).

broadening in the film to the strong coupling effect of the LSPR of neighboring AuNRs due to the exceptionally high content of AuNRs in the NIMs (75% wt).<sup>[44,45]</sup> Note that there is no additional solvent in the NIMs film, since the particles are self-suspended. In addition, the surface functionalization of AuNRs

with MPS-Jeffamine macromolecules may also contribute to the broadening of the SPR peak.<sup>[46]</sup> Figure 2f shows the polarized absorption spectra of the aligned AuNR NIMs film. The absorbance peak around 1300 nm corresponds to the longitudinal SPR of the AuNRs. The intensity of the absorbance



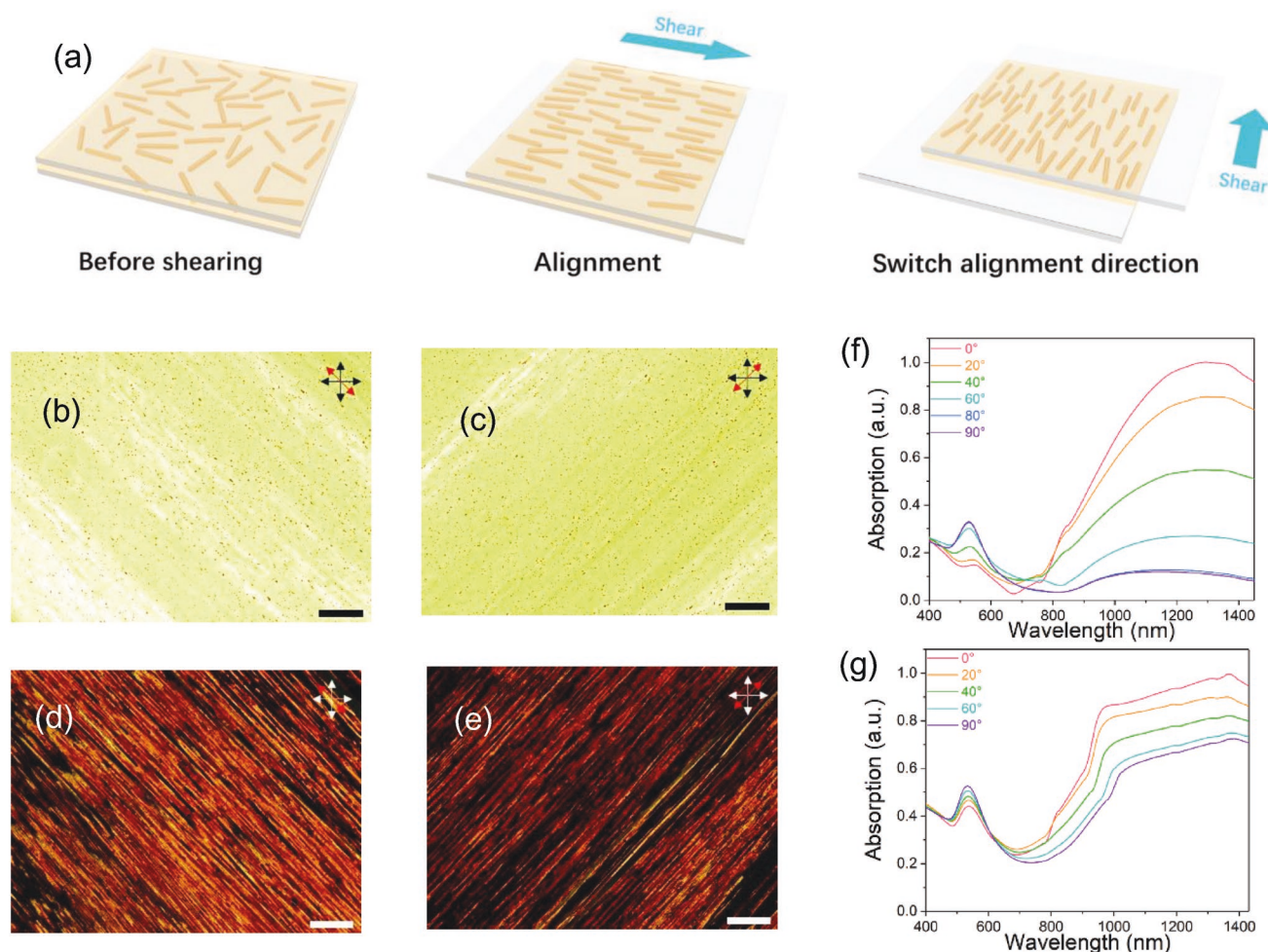


**Figure 2.** a) Schematics showing switchable alignment of AuNR NIMs. b,c) Polarized optical microscope images of the AuNR NIMs film (scale bar is 200  $\mu\text{m}$ ) before and after changing the shearing direction. d,e) Polarized optical microscope images of the aligned control film (scale bar = 100  $\mu\text{m}$ ) before and after changing alignment. f,g) Polarized UV-vis-NIR spectra of the aligned films of AuNR NIMs and the control containing 75 wt% of AuNRs.

peak reached a maximum, when the angle between the polarizer and the shearing direction was 0°. The absorbance gradually decreased to the minimum at 90°, where the intensity decreased by 90% of that at 0°. In contrast to the longitudinal SPR of the AuNRs, the transverse SPR peak around 530 nm exhibited a much less pronounced, reverse change in intensity with the rotation angle of the polarizer. These results confirm that the majority of the AuNRs in the NIMs film are aligned along the shearing direction. An alignment index of AuNRs can be estimated using the 3D order parameter  $S_{3D}$ , which can be calculated by the following equation

$$S_{3D} = \frac{A_{\parallel} - A_{\perp}}{A_{\parallel} + 2A_{\perp}} \quad (1)$$

where  $A_{\parallel}$  and  $A_{\perp}$  are the corresponding absorbance at angles of 0° and 90° between the polarizer and the shearing direction, respectively.<sup>[30]</sup> The calculated  $S_{3D}$  of the aligned AuNR NIMs film is 0.72, which is among the highest compared with the previously reported results using only shearing protocols.<sup>[28,30]</sup> While the order parameter of the AuNR NIMs is comparable

to other highly ordered AuNRs system our system contains an order of magnitude higher content of AuNRs.<sup>[30]</sup> In contrast to the AuNR NIMs film, the film prepared using the control (non-ionic) sample showed much lower  $S_{3D} \approx 0.13$ , indicating again the critical nature of the ionic interactions for alignment. The order parameter of the AuNR NIMs film remained the same after storage at room temperature for over a month (Figure S4b, Supporting Information), showing consistency with high stability of the alignment. To the best of our knowledge, this is the first report of large area switchable alignment of AuNRs with high orientational tunability and stability.

The critical role of ionic interaction in AuNR NIMs versus the control sample is confirmed by rheological measurements. Figure 3a shows the temperature-dependent rheological behavior of AuNR NIMs and the nonionic control. After heating to 70 °C for 1 min, the storage and loss moduli of the control increased by nearly 30 fold when the temperature decreased from 70 to 25 °C. A similar trend was also found in their complex viscosity. For the control sample, because of the absence of the ionic interaction between sulfonated AuNRs and the Jeffamine polymer, the AuNRs showed a tendency to agglomerate

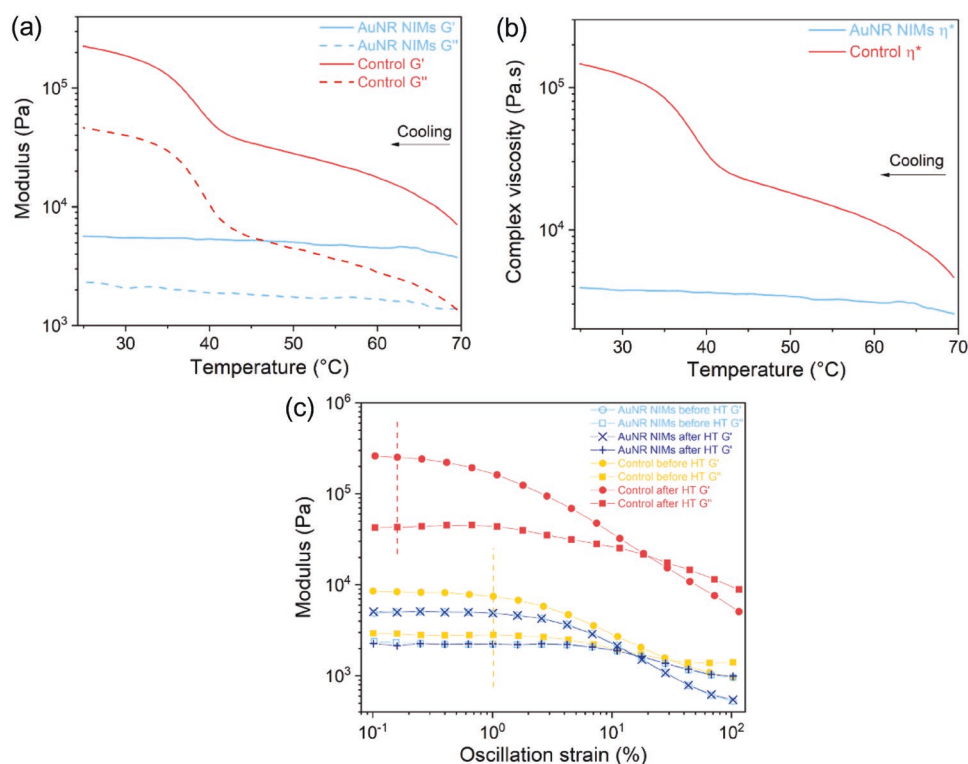


**Figure 3.** a) Temperature dependence of the storage and loss modulus for AuNR NIMs, and the nonionic control sample. The latter is synthesized from the Na form of MPS functionalized AuNRs and Jeffamine. b) Temperature dependence of the complex viscosity for AuNR NIMs and the control. c) Modulus–strain curves for AuNR NIMs and the control before and after HT at 70 °C. Dotted lines show the end of linear region for AuNR NIMs and the control before and after heat treatment.

upon heat treatment (HT) and shearing, resulting in much higher modulus and viscosity. This assertion is also supported by comparing the modulus–strain curves in Figure 3c. The control showed a shorter linear region followed by a non-linear region with an increasing slope after heat treatment. Much higher storage and loss moduli observed after the heat treatment can be attributed to solid-like rheological behavior induced by AuNR agglomerates. Compared with the control, no change in modulus was found for the AuNR NIMs before and after heat treatment, indicating excellent stability of the sample against aggregation.

Based on the liquid crystal behavior of AuNR NIMs, we speculated that the film would exhibit anisotropic conductivity. The DC conductivities of the AuNR NIMs film in the directions parallel and perpendicular to the alignment were compared by measuring the resistance of the sample sheared between two parallel gold pads (Figure 4a,b). Resistance was measured using a Keithley 2400 multimeter and a Keyence VK-X260 laser scanning confocal microscope was used to measure the dimensions and average thickness of the film (Figure 4c). Three separate samples were prepared using the same protocol and multiple measurements were taken at several places in each sample to account for the errors and deviations which can be caused during the sample preparation. The conductivity of AuNR NIMs is  $\sigma_{\parallel} = 1.5 \pm 0.2 \times 10^{-5} \text{ S cm}^{-1}$  and  $\sigma_{\perp} = 1.8 \pm 1.0 \times 10^{-6} \text{ S cm}^{-1}$  for the directions parallel and perpendicular to the alignment, respectively. Note that the conductivity of AuNR NIMs before shearing is  $5.2 \pm 0.3 \times 10^{-6} \text{ S cm}^{-1}$ . Despite the errors in  $\sigma_{\parallel}$

and  $\sigma_{\perp}$ , the conductivity is consistently higher in the direction parallel to the shear. Also, regardless of the presence of the electrically insulating polymer layer surrounding the conductive AuNRs, the overall conductivity is in the range of doped organic semiconductors.<sup>[47]</sup> We believe that the alignment of AuNRs influences the morphology of the canopy molecules in a way that a percolative current path can be easily created, which results in the anisotropic conductivity of the AuNR NIMs film. This anisotropic conductivity of AuNR NIMs might be useful for potential application in ultrathin shear sensors.

In summary, this paper demonstrates a new solvent free, high inorganic content lyotropic liquid crystal with high tunability and stability of alignment based on AuNR NIMs. A simple and scalable shearing protocol allows for alignment and realignment of the AuNRs in the NIMs films. This is the first example of a switchable, colloidal plasmonic nanorods system containing as high as 75 wt% of inorganic content. The AuNR NIMs also exhibited remarkable stability and retained alignment for months after shearing. The unidirectional ordering of AuNRs with an order parameter reaching 0.72 was confirmed by UV–vis spectroscopy, showing the strong polarization sensitivity due to the SPR effect. The rheological behavior of AuNR NIMs was contrasted to a control sample of similar composition without the ionic interaction between the corona and the canopy, and the differences were attributed to the lack of aggregation in the ionic system compared to the control. The alignment of AuNRs also results in anisotropic conductivity with an order of magnitude difference between the

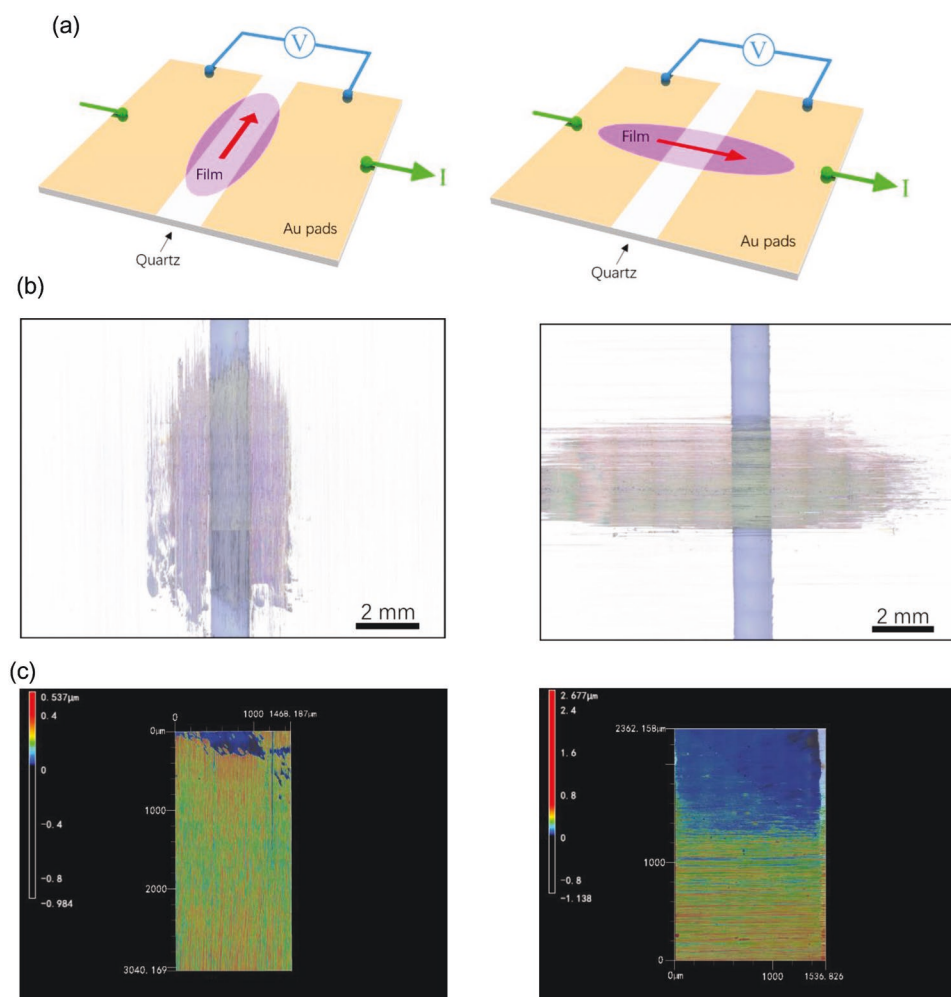


**Figure 4.** a) Schematic representation showing the patterns used for resistance measurement of AuNR NIMs film. The red arrows show the directions of alignment for AuNRs. b) Photos of the AuNR NIMs films in the resistance measurement. c) 3D maps of thickness profile for the AuNR NIMs film obtained from confocal laser scanning microscope.

conductivities in directions parallel and perpendicular to the alignment. The AuNR NIMs system might be applicable in a wide range of applications, where device-scale film alignment is required, including tunable linear-polarized light emitters and tunable polarizer filters, tunable diodes, shear sensors, and stretch detectors.

## Experimental Section

**Materials:** Silver nitrate ( $\text{AgNO}_3$ , 99%), gold(III) chloride trihydrate ( $\text{HAuCl}_4 \cdot 3\text{H}_2\text{O}$ , 99.9%), sodium borohydride ( $\text{NaBH}_4$ , 99%), L-ascorbic acid (AA, 99.0%), MPS (90%), poly(sodium 4-styrene-sulfonate) (PSS,  $M_w = 70\,000$ ), and Dowex Marathon C cation exchange resin were purchased from Sigma-Aldrich. Sodium oleate (NaOL, 97%) and CTAB (98%) were obtained from Tokyo Chemical Industry. Jeffamine M-2070 polyetheramine (Jeffamine) was obtained from Huntsman. Hydrochloric acid was purchased from VWR International. All chemicals were used as received without further purification. Millipore Milli-Q water (resistivity  $> 18\,\text{M}\Omega\,\text{cm}^{-1}$  at  $25\,^\circ\text{C}$ ) was used in all the experiments.

**Characterization:** UV absorption spectra were acquired on a Cary 5000 UV-vis-NIR spectrophotometer (Agilent Technologies, USA). TEM images were taken on a FEI F20 TEM STEM (Philips, Dutch)

microscope. Zeta potential was obtained from a Nano 90 zetasizer (Malvern Panalytical, UK). TGA data were acquired on a TGA Q500 (TA instrument, USA) with a ramp rate of  $10\,^\circ\text{C}\,\text{min}^{-1}$  in  $\text{N}_2$  from  $30$  to  $800\,^\circ\text{C}$ . Rheological measurements were obtained on a DHR3 Rheometer (TA instrument, USA). Materials were placed onto an 8 mm parallel plate fixture and maintained at  $25\,^\circ\text{C}$ . The gap distance was set to  $100\,\mu\text{m}$ . A temperature sweep from  $70$  to  $25\,^\circ\text{C}$  with a ramp rate of  $1\,^\circ\text{C}\,\text{min}^{-1}$  was performed with a soak time of  $60\,\text{s}$  after reaching  $70\,^\circ\text{C}$ . The strain was set at  $0.25\%$  and the frequency at  $0.25\,\text{Hz}$ . Strain sweep was measured by varying the strain from  $0.1\%$  to  $100\%$  at a frequency of  $0.25\,\text{Hz}$ . The shear rate sweep was measured from  $0.1$  to  $100\,\text{s}^{-1}$  and the strain was set at  $0.03\%$ . Optical microscope images were obtained with an Infinity 3 (Lumenera corporation, Canada) microscope. Conductivity measurements were performed using a Keithley 2400 SourceMeter (Figure S5, Supporting Information). Substrates for the conductivity measurements were produced by evaporating Cr/Au layer on quartz substrate using shadow mask and CVC SC4500 combination thermal/ E-gun Evaporation System. The thickness of the films was measured using a Keyence VK-X206 Laser-Scanning Confocal Microscope (Keyence, Japan) by mapping out the thickness profile in 3D and averaging the height. Length and width of the film was determined from the optical image taken from the same confocal microscope. The surface chemical elements of AuNRs were determined by XPS.



**Synthesis—Synthesis of AuNRs:** AuNRs were prepared using the seeded growth approach as previously described and briefly presented below.<sup>[40]</sup>

**Preparation of AuNR Seeds:** A freshly prepared NaBH<sub>4</sub> solution ( $6 \times 10^{-3}$  M, 1 mL) was added to a solution containing HAuCl<sub>4</sub> ( $0.5 \times 10^{-3}$  M, 5 mL) and CTAB (0.2 M, 5 mL) under vigorous stirring (1200 rpm). After stirring for 2 min, the obtained seed solution was aged for 30 min at room temperature.

**Growth of AuNRs:** CTAB ( $7.68 \times 10^{-3}$  M) and sodium oleate (NaOL,  $1.62 \times 10^{-3}$  M) were dissolved in 100 mL of water at 50 °C. AgNO<sub>3</sub> ( $4 \times 10^{-3}$  M, 9.6 mL) and HAuCl<sub>4</sub> ( $1 \times 10^{-3}$  M, 100 mL) were added to the CTAB/NaOL solution and the mixture was kept undisturbed at 30 °C for 15 min. After stirring at 700 rpm for 90 min, the solution became colorless. HCl (37%, 2.16 mL) was then introduced to the solution and kept stirring at 400 rpm for 15 min. Subsequently, ascorbic acid (0.5 mL,  $64 \times 10^{-3}$  M) was added and the solution was vigorously stirred for 30 s. In the end, the seed solution (0.8 mL) was injected and then stirred for 30 s. The mixture left undisturbed at 30 °C for 12 h. The solution was centrifuged at 8000 rpm for 30 min to get the AuNRs.

**Synthesis—Preparation of PSS-Stabilized AuNRs (PSS-AuNRs):** The concentration of CTBA in AuNRs solution was reduced to  $1 \times 10^{-3}$  M by centrifugation (8000 rpm, 30 min) and redispersion in water.<sup>[41]</sup> The retentate was redispersed in 0.7 wt% PSS solution (O.D.>10) and kept for 1–2 h. The solution was centrifuged at 8000 rpm for 30 min. The supernatant was decanted and the retentate was redispersed in 0.7% PSS solution. The centrifugation-redispersion cycle was repeated twice to remove residual CTAB.

**Synthesis—Synthesis of MPS/Jeffamine Ligand (Corona-Canopy Salt for NIMs):** MPS (0.1 M, 10 mL) was fully protonated via ion exchange using Dowex Marathon C cation exchange resin and then mixed with the Jeffamine aqueous solution (0.1 M, 10 mL). The mixture was shaken for 30 min before 30 min sonication.

**Synthesis—Preparation of AuNR NIMs:** AuNRs suspended in 0.7 wt% PSS was centrifuged (8000 rpm, 30 min) and the supernatant was decanted until 0.2 mL of retentate remained. The retentate was redispersed in 5 mL of water. The NIMs ligand solution was added and sonicated for 1 min. The obtained solution was kept at room temperature for 24 h and then freeze dried to get a dark purple viscous nanocomposite.

The control sample was prepared following the synthesis of AuNR NIMs described above except that the corona/canopy ligand solution was replaced by a solution of sodium 3-mercapto-1-propanesulfonate (0.1 M, 10 mL) mixed with the Jeffamine aqueous solution (0.1 M, 10 mL). The presence of the Na ions prevented the formation of the sulfonate/ammonium salt described above.

## Supporting Information

Supporting Information is available from the Wiley Online Library or from the author.

## Acknowledgements

X.L. and G.Q. contributed equally to this work. This work made use of the Cornell Center for Materials Research Shared Facilities which are supported through the NSF MRSEC program (DMR-1719875). This work was performed in part at Cornell NanoScale Facility, an NNCI member supported by NSF Grant NNCI-1542081. The authors thank Michael A. Rutzke for ICP measurement. This work was performed in part at Cornell Energy Systems Institute.

## Conflict of Interest

The authors declare no conflict of interest.

## Keywords

anisotropic conductivity, gold nanorods, liquid crystals, switchable and stable alignment, thin films

Received: April 1, 2019  
Published online: April 25, 2019

- [1] Y. H. Su, Y. F. Ke, S. L. Cai, Q. Y. Yao, *Light: Sci. Appl.* **2012**, *1*, e14.
- [2] Q. F. Zhang, E. Uchaker, S. L. Candelaria, G. Z. Cao, *Chem. Soc. Rev.* **2013**, *42*, 3127.
- [3] S. Linic, P. Christopher, D. B. Ingram, *Nat. Mater.* **2011**, *10*, 911.
- [4] W. F. Paxton, K. C. Kistler, C. C. Olmeda, A. Sen, S. K. St. Angelo, Y. Y. Cao, T. E. Mallouk, P. E. Lammert, V. H. Crespi, *J. Am. Chem. Soc.* **2004**, *126*, 13424.
- [5] M. C. Daniel, D. Astruc, *Chem. Rev.* **2004**, *104*, 293.
- [6] Y. Zhang, X. J. Cui, F. Shi, Y. Q. Deng, *Chem. Rev.* **2012**, *112*, 2467.
- [7] S. Link, M. A. El-Sayed, *J. Phys. Chem. B* **1999**, *103*, 8410.
- [8] M. B. Mohamed, V. Volkov, S. Link, M. A. El-Sayed, *Chem. Phys. Lett.* **2000**, *317*, 517.
- [9] N. J. Durr, T. Larson, D. K. Smith, B. A. Korgel, K. Sokolov, A. Ben-Yakar, *Nano Lett.* **2007**, *7*, 941.
- [10] X. H. Huang, I. H. El-Sayed, W. Qian, M. A. El-Sayed, *J. Am. Chem. Soc.* **2006**, *128*, 2115.
- [11] G. V. Maltzahn, J. H. Park, A. Agrawal, N. K. Bandaru, S. K. Das, M. J. Sailor, S. N. Bhatia, *Cancer Res.* **2009**, *69*, 3892.
- [12] E. C. Dreaden, A. M. Alkilany, X. H. Huang, C. J. Murphy, M. A. El-Sayed, *Chem. Soc. Rev.* **2012**, *41*, 2740.
- [13] S. Eustis, M. A. El-Sayed, *Chem. Soc. Rev.* **2006**, *35*, 209.
- [14] H. J. Chen, L. Shao, Q. Li, J. F. Wang, *Chem. Soc. Rev.* **2013**, *42*, 2679.
- [15] M. A. Boles, M. Engel, D. V. Talapin, *Chem. Rev.* **2016**, *116*, 11220.
- [16] S. Y. Zhang, M. D. Regulacio, M. Y. Han, *Chem. Soc. Rev.* **2014**, *43*, 2301.
- [17] M. Schnell, A. Garcia-Etxarri, A. J. Huber, K. Crozier, J. Aizpurua, R. Hillenbrand, *Nat. Photonics* **2009**, *3*, 287.
- [18] P. H. Li, Y. Li, Z. K. Zhou, S. Y. Tang, X. F. Yu, S. Xiao, Z. Z. Wu, Q. L. Xiao, Y. T. Zhao, H. Y. Wang, P. K. Chu, *Adv. Mater.* **2016**, *28*, 2511.
- [19] K. Kim, H. S. Han, I. Choi, C. W. Lee, S. Hong, S.-H. Suh, L. P. Lee, T. Kang, *Nat. Commun.* **2013**, *4*, 2182.
- [20] R. A. Alvarez-Puebla, A. Agarwal, P. Manna, B. P. Khanal, P. Aldeanueva-Potel, E. Carbo-Argibay, N. Pazos-Perez, L. Vigderman, E. R. Zubarev, N. A. Kotov, L. M. Liz-Marzan, *Proc. Natl. Acad. Sci. USA* **2011**, *108*, 8157.
- [21] C. Hamon, S. Novikov, L. Scarabelli, L. Basabe-Desmonts, L. M. Liz-Marzan, *ACS Nano* **2014**, *8*, 10694.
- [22] B. Peng, G. Y. Li, D. H. Li, S. Dodson, Q. Zhang, J. Zhang, Y. H. Lee, H. V. Demir, X. Y. Ling, Q. H. Xiong, *ACS Nano* **2013**, *7*, 5993.
- [23] Y. Zhang, Q. K. Liu, H. Mundoor, Y. Yuan, I. I. Smalyukh, *ACS Nano* **2015**, *9*, 3097.
- [24] Z. Yin, D. L. Zhou, W. Xu, S. B. Cui, X. Chen, H. Wang, S. H. Xu, H. W. Song, *ACS Appl. Mater. Interfaces* **2016**, *8*, 11667.
- [25] Q. Q. Tong, E. W. Malachosky, J. Raybin, P. Guyot-Sionnest, S. J. Sibener, *J. Phys. Chem. C* **2014**, *118*, 19259.
- [26] V. Flauraud, M. Mastrangeli, G. D. Bernasconi, J. Butet, D. T. L. Alexander, E. Shahrabi, O. J. F. Martin, J. Brugger, *Nat. Nanotechnol.* **2017**, *12*, 73.
- [27] M. Tebbe, M. Mayer, B. A. Glarz, C. Hanske, P. T. Probst, M. B. Muller, M. Karg, M. Chanana, T. A. F. Konig, C. Kuttner, A. Fery, *Faraday Discuss.* **2015**, *181*, 243.
- [28] X. Feng, L. Sosa-Vargas, S. Umadevi, T. Mori, Y. Shimizu, T. Hegmann, *Adv. Funct. Mater.* **2015**, *25*, 1180.

- [29] B. Rozic, J. Fresnais, C. Molinaro, J. Calixte, S. Umadevi, S. Lau-Truong, N. Felidj, T. Kraus, F. Charra, V. Dupuis, T. Hegmann, C. Fiorini-Debuisschert, B. Gallas, E. Lacaze, *ACS Nano* **2017**, *11*, 6728.
- [30] Q. K. Liu, Y. X. Cui, D. Gardner, X. Li, S. L. He, I. I. Smalyukh, *Nano Lett.* **2010**, *10*, 1347.
- [31] M. R. Jones, R. J. Macfarlane, B. Lee, J. Zhang, K. L. Young, A. J. Senesi, C. A. Mirkin, *Nat. Mater.* **2010**, *9*, 913.
- [32] S. Sekar, V. Lemaire, H. Hu, G. Decher, M. Pauly, *Faraday Discuss.* **2016**, *191*, 373.
- [33] X. J. Zan, S. Feng, E. Balizan, Y. Lin, Q. Wang, *ACS Nano* **2013**, *7*, 8385.
- [34] R. Rodriguez, R. Herrera, L. A. Archer, E. P. Giannelis, *Adv. Mater.* **2008**, *20*, 4353.
- [35] A. B. Bourlinos, R. Herrera, N. Chalkias, D. D. Jiang, Q. Zhang, L. A. Archer, E. P. Giannelis, *Adv. Mater.* **2005**, *17*, 234.
- [36] N. J. Fernandes, J. Akbarzadeh, H. Peterlik, E. P. Giannelis, *ACS Nano* **2013**, *7*, 1265.
- [37] R. Rodriguez, R. Herrera, A. B. Bourlinos, R. P. Li, A. Amassian, L. A. Archer, E. P. Giannelis, *Appl. Organomet. Chem.* **2010**, *24*, 581.
- [38] M. L. Jespersen, P. A. Mirau, E. V. Meerwall, R. A. Vaia, R. Rodriguez, E. P. Giannelis, *ACS Nano* **2010**, *4*, 3735.
- [39] R. R. Bhattacharjee, R. P. Li, L. Estevez, D. M. Smilgies, A. Amassian, E. P. Giannelis, *J. Mater. Chem.* **2009**, *19*, 8728.
- [40] X. C. Ye, Zheng, C. Zheng, J. Chen, Y. Z. Gao, C. B. Murray, *Nano Lett.* **2013**, *13*, 765.
- [41] J. G. Mehtala, D. Y. Zemlyanov, J. P. Max, N. Kadasala, S. Zhan, A. Wei, *Langmuir* **2014**, *30*, 13727.
- [42] A. P. Leonov, J. W. Zheng, J. D. Clogston, S. T. Stern, A. K. Patri, A. Wei, *ACS Nano* **2008**, *2*, 2481.
- [43] D. Sahu, H. C. Chu, P. J. Yang, H. C. Lin, *Macromol. Chem. Phys.* **2012**, *213*, 1550.
- [44] J. Zhu, S. W. Bai, J. W. Zhao, J. J. Li, *Appl. Phys. A* **2009**, *97*, 431.
- [45] J. Sancho-Parramon, *Nanotechnology* **2009**, *20*, 235706.
- [46] M. Jebb, P. K. Sudeep, P. Pramod, K. G. Thomas, P. V. Kamat, *J. Phys. Chem. B* **2007**, *111*, 6839.
- [47] A. Nollau, M. Pfeiffer, T. Fritz, K. Leo, *J. Appl. Phys.* **2000**, *87*, 4340.